Environmental Science Nano

ARTICLE

Received 00th January 20xx,
Accepted 00th January 20xx

DOI: 10.1039/x0xx00000x
www.rsc.org/

Biodegradation of graphene oxide-polymer nanocomposite films in wastewater

Jingjing Fan[a], Carlos David Grande[b], Debora F. Rodrigues[a*]

The synthesis of polymer nanocomposites has been extensively investigated by many researchers, however, the end of life fate of polymer nanocomposites is still largely unknown. It is expected that at the end of their service life, these polymer nanocomposites will most likely end up in soil and water systems where microorganisms will interact and, perhaps, even biodegrade them. In this study, we investigate the ability of wastewater microorganisms to biodegrade nanocomposite films containing different graphene oxide (GO) loads (0% to 0.6%, (w/w%)) embedded in a model biopolymer (*i.e.* chitosan). The ability of wastewater microorganisms to grow and form biofilms on the surface of the nanocomposite films was determined by live and dead staining assisted with confocal laser scanning microscopy. The capability of wastewater biofilms to biodegrade nanocomposites was assessed through nanocomposite film weight losses, Fourier transformed infrared (FTIR) and Scanning electron microscopy (SEM) analyses. Results showed that microorganisms present in the activated sludge can grow on the surface of the nanocomposites and biodegrade the polymer surrounding the graphene oxide nanoplatelets. As the biopolymer gets degraded, there is increasing exposure of GO on the surface, which yields microbial inactivation and biofilm growth inhibition. To determine the evolution of the toxicity of the nanocomposite during biodegradation. We determined the emergence of the sharp edges of GO on the surface of the nanocomposite through atomic force microscopy (AFM), as well as the production of reactive oxygen species (ROS) with the Ellman's assay before and after biodegradation of the nanocomposites. The results show that as GO surfaces the nanocomposite film during biodegradation, there is increasing production of ROS, which explains the increasing inactivation of the microorganisms.

Keywords: Chitosan, Graphene Oxide, Biodegradation, Wastewater, nanocomposites

Nano impacts

This study presents for the first time the end-of-life fate of biopolymer graphene oxide nanocomposites in the environment. In the present investigation, environmental microorganisms were demonstrated to be able to biodegrade polymers surrounding the nanomaterial graphene oxide embedded in the nanocomposites. During biodegradation of the polymer, however, the nanoparticles were exposed to the environment and led to microbial inactivation. This study helps to understand the fate of graphene oxide nanocomposites at the end of their life cycle. Furthermore, this study brings a new direction to research on nanocomposite biodegradation and environmental implications of nanocomposites.

[a] *Department of Civil and Environmental Engineering, University of Houston, Houston, TX 77204-4003 (USA)*
[b] *Department of Chemistry, Universidad del Atlántico, Puerto Colombia, Atlantico 8000-1 (Colombia)*
[a*] *Corresponding Author: Dr. Debora F. Rodrigues dfrigirodrigues@uh.edu;*
† Footnotes relating to the title and/or authors should appear here.
Electronic Supplementary Information (ESI) available: [details of any supplementary information available should be included here]. See
DOI: 10.1039/x0xx00000x

Introduction

Nanocomposites are advanced functional materials composed of nanomaterials dispersed inside polymer matrices. To date, extensive studies have demonstrated that nanocomposites can show great mechanical, water resistance, and antimicrobial properties, depending on the concentration of the nanomaterial embedded in the nanocomposite.[1, 2] These advanced composite materials are being increasingly used in many industries, including consumer products.[3, 4] However, the long-term performance of the nanocomposite product itself and the fate of nanocomposites and nanoparticles after disposal play an essential role in the public acceptance and commercialization of these advanced materials. For most commercial products, it is expected that the materials will undergo degradation during the service and post-service life (e.g. landfills and wastewater treatment). In the case of nanocomposites, the fate and post-service life are still largely unknown. As for most materials, it is expected that these nanocomposites will suffer some sort of degradation at the end of their life-cycle.

Degradation is a process where the deterioration in the properties of the polymer takes place due to different factors like, photocatalysis as well as hydrolytic, thermal and microbial degradation.[5] As a consequence of degradation, the resulting material will not present the same properties as the original material.[6] Hence, a better understanding of degradation mechanisms of a material will ensure its use in applications that will allow an increase in the material life spam, as well as identification of better disposal mechanisms to reduce potential environmental impacts. So far, not enough attention has been given to degradation of nanocomposites as compared to their preparation techniques and evaluation of their application properties.

This study aims to investigate the microbial degradation of nanocomposites to simulate the fate of nanocomposites at the end of their life-cycle. More specifically, in this study, we evaluate the biodegradation of a graphene oxide biopolymer nanocomposite. We embedded different concentrations of graphene oxide in a model biopolymer, chitosan (β-(1,4)-2-amino-2-deoxy-d-glucopyranose), to synthesize nanocomposites with different GO loads. Chitosan was selected as the model biopolymer, because is extensively used in different industries, is biodegradable and cheap. Additionally, several studies have shown that the incorporation of GO into chitosan enhances significantly the material properties, such as thermal, mechanical and antimicrobial properties of chitosan, making this material extremely valuable for different biomedical, food packaging and environmental applications.[2, 7-9] In the present study, the biodegradation of the nanocomposite was investigated with activated sludge bacterial community to provide insights about the end of life behavior of nanocomposites.

Experimental

CS-GO nanocomposite preparation and characterization

The GO used in this study was from the same batch as our previous published study.[10] Detailed information about the preparation and characterization of GO used in this study can be found in our recently published study.[10] The preparation of the chitosan-graphene oxide nanocomposite films (CS-GO) is also described in detail in our previously published studies.[12-14] Briefly, chitosan was dissolved in glacial acetic acid solution (1% v/v) to obtain a 2% (w/v) solution. A clean solution of chitosan was obtained through filtration (Whatman No. 3 filter paper, 125 mm diameter, SKU 1003-125). This solution was added to a GO suspension. After 1 h sonication, a homogeneous solution was obtained using the ultraturrax, and then sonicated at 60°C for 1 h. The CS-GO solution was then poured onto a glass plate and dried overnight at room temperature. After drying, CS-GO nanocomposite films were peeled off and left under vacuum for thermal post-crosslinking at 120 °C. Nanocomposite films with 0.25 wt% and 0.6 wt% of GO loadings (coded as CS-GO-0.25, and CS-GO-0.6) were selected for this investigation, while CS films without GO served as controls. Nanocomposite films characterization and their physicochemical properties were investigated through Fourier Infrared Spectroscopy (FTIR), Atomic force microscopy (AFM), Contact angle measurement, thermogravimetric analysis (TGA), Gel content, and Differential scanning calorimetry (DSC), and presented in the supporting information (Figure S1,S2, S3, S4, S5, S6).

Wastewater collection and synthetic wastewater preparation

The original activated sludge was obtained from the aeration tank of Sims South Bayou Wastewater Treatment Plant (Houston, TX) and kept in a long-term (110 days) 4 L sequencing batch reactor. To keep the activated sludge alive, air was provided by an air pump with 5 L/min through aeration diffusers placed at the bottom of the container, and the temperature was kept at 23±2℃. The pH was adjusted and kept at 7.5 using $NaHCO_3$ solution. The bioreactor had a daily cycle of 8 h with 6 h of aeration, 0.5 h settling, 0.5 h of drawing and 1 h idle, and a total 60 cycles as an acclimation period. A volume of 2L of synthetic wastewater was added to the reactor at the end of every cycle to supply enough nutrients to the activated sludge after taking out the same amount of water from the reactor.

The composition of the synthetic wastewater was 330 mg/L of NH_4^+, and 37.6 mg/L of PO_4^{3+}. The trace element solution contained 15 mg/L of EDTA, 5 mg/L of $FeSO_4 \cdot 7H_2O$, 0.05 mg/L of $NiCl_2 \cdot 6H_2O$, 0.06 mg /L of $CuSO_4 \cdot 5H_2O$, 0.06 mg/L of $CoCl_2 \cdot 6H_2O$, 0.10 mg/L of $ZnSO_4 \cdot 7H_2O$, 0.10 mg/L of $NaMoO_4 \cdot 2H_2O$, 0.28 mg/L of $MnCl_2 \cdot 4H_2O$, 0.05 mg/L of $NaSeO_4 \cdot 10H_2O$, and 0.014 mg/L of H_3BO_3. The synthetic wastewater had a COD of 1000 mg/L. [15]

Biofilm growth on nanocomposite films

The biofilm growth on CS-GO films were investigated by depositing six replicate films of CS-GO films at the bottom of 6 well flat-bottom microtiter plates (Costar 3370, Corning, NY). A volume of 4 mL of wastewater sludge was inoculated into the wells and incubated under static conditions for 3 to 6 d to allow mature biofilms to form on the surface of the films. A volume of 1 mL fresh synthetic wastewater was added to each well every 24 h after taking the same volume from the wells. This procedure aimed to ensure the presence of enough nutrients for the microorganisms to grow. Films of chitosan without nanomaterials incubated with sludge were used as positive controls. Negative controls contained the CS and nanocomposite films with sterile synthetic wastewater without sludge. After 3 d of incubation, three films were taken out from microtiter plates, gently washed with DI water to remove excess sludge and analysed with confocal microscopy for biofilm growth. The same films were further analysed for other changes in their surface properties as described below. The other three films in the microtiter plates were continuously exposed to wastewater until 6 d. After this period, the films were analysed following the same procedures as the films incubated for 3 d.

Confocal microscopy and image analysis

The biofilm formed on the films were analysed with confocal laser microscopy (CLSM) (Leica Lasertechnik, Heidelberg, Germany). After 3 and 6 d, the nanocomposites and chitosan films were analysed to determine the total amount of live and dead cells in the biofilms on top of the films. The biofilms were stained with a live/dead Baclight bacterial viability kit (Invitrogen).[12] This kit

employs two nucleic acid dyes: SYTO 9 and propidium iodide (PI). SYTO 9 will stain all cells with green colour, while PI will stain in red the cells with damaged membranes. The stained biofilms were observed by CLSM with a 10X objective lens. Fluorescence images were taken at excitation and emission wavelengths of 535 nm and 617 nm, respectively, for the PI dye. For the SYTO 9, the images were observed at excitation and emission wavelengths of 485 nm and 495 nm, respectively. In all experiments, three stack images were acquired at random positions of the sample with 2 µm intervals from the nanocomposite films through the top of the biofilms. The thickness of the biofilms was determined by adding up all slices of the stack images. The 3-dimensional projections of the biofilm structure were reconstructed from z-stakes using Image J. COMSTAT software was used to calculate the total biomass, dead biomass, and the average thickness of the biofilms.[16] Inactivation percentage of cells in the biofilm was calculated by using the dead biomass, as indicated by the red colour of the PI stain, divided by the total biomass. The standard deviations for all analyses were calculated with excel and plotted in the graphs as error bars.

CS-GO films surface analyses after interaction with biofilm

The dry weight (W_o) of the nanocomposite was measured with an analytical balance (Mettler Toledo s6, United States) before exposure to wastewater and after 3 and 6 d of incubation with the sludge. The films exposed to sterile wastewater sludge were used as negative controls. The biofilm on top of the nanocomposite films were removed physically with a humid Kimwipe (KIMTECH SCIENCE* KIMWIPES, Kimberly-Clark Professional, USA) to allow more accurate surface analysis. The controls were wiped using the same procedure. The treated films were dried at room temperature for 48 h and weighted again as W_1. The weight loss was calculated as a percentage of the original sample weight (W_o). Averages of triplicate samples and their respective standard deviations were calculated with excel.

$$\text{Weight loss (\%)} = \frac{(W_0 - W_1)}{W_0} \times 100\%$$

Infrared spectra were used to identify the changes in functional groups on the chitosan and CS-GO films before and after interaction with the wastewater bacterial community. The treated films were analysed with the Nicolet iS10 Mid Infrared FT-IR Spectrometer (Thermo Fisher Scientific) equipped with ZnSe crystal and the Omnic 8 Software (Thermo Fisher Scientific). The infrared spectrum for each sample was recorded in the range of 4000-400 cm^{-1} with a resolution at 4 cm^{-1}.[17] The background noise of atmospheric water and CO_2 was automatically subtracted from all spectra.

The surface roughness of the nanocomposites was measured by *ex situ* Atomic Force Microscopy (AFM) measurements. AFM tapping mode (AFM, Veeco, Inc) was used at a scan rate of 1.0 Hz. The height, amplitude, and phase images were collected simultaneously. Probes used were 125 µm long with antimony doped silicon tips (TESPA, Brukeprobes). The drive frequency was 320 kHz, and the typical spring constant was 42 N/m. NanoScope Analysis 1.5 was used to get the topographic information of the samples, and to analyse the roughness of the collected images.

The surface morphology of the nanocomposites was visualized through Scanning Electron Microscopy (SEM). Dried films were sputter coated with gold (Denton Desk V HP, Beijing, China) and SEM images were acquired in Field-emission SEM (FESEM; LEO 1525, Oberkochen, Germany).

Thiol Oxidation and Quantification

The oxidation of thiol groups in the glutathione (GSH) molecules exposed to the nanocomposite films, before and after incubation with wastewater, were quantified by the Ellman's assay. The procedure was described in detail in our previous publication.[4] Briefly, the chitosan films loaded with different concentrations of GO were placed into 2 mL tubes. A volume of 225 µL of GSH (0.4 mM in 50 mM bicarbonate buffer) was added to tubes to initiate reaction. The negative control was the GSH solution only, without interaction with the nanocomposites; while GSH oxidization by H_2O_2 (30%) was used as a positive control. All the samples were incubated at room temperature for 2 h with 150 rpm mixing. After incubation, 785 µL of 0.05 M Tris-HCl and 15 µL of DNTB (Ellman's reagent, 5,5'-dithio-bis-(2-nitrobenzoic acid), Sigma-Aldrich) were added into the liquid solution to yield a yellow product. All the samples were incubated for 10 min in the dark, and then filtered through 0.2 µm pore size membrane filters (PTFE Milipore filter, KTGR04FH3). A 250 µL volume of each filtrate was transferred into a 96-well microtiter plate and the absorbance was measured at 412 nm using Synergy MX Microtiter plate reader (Biotek, U.S.A). The loss of GSH in each sample was calculated by the following formula:

$$\%\ \text{GSH loss} = \frac{(\text{absorbance of negative control} - \text{absorbance of sample})}{\text{absorbance of negative sample}} \times 100$$

Statistical analysis

Each set of experiments were carried out in triplicate. For all results, average and standard deviations were calculated in excel and plotted in the graphs. Further statistical analyses were performed using unpaired t-test to determine statistically the difference for loss of glutathione among the controls, CS-GO 0.25% and CS-GO 0.6%.

Results and discussion

Biofilm growth on the surface of GO nanocomposite films

The successful preparation and characterization of the nanocomposites of CS-GO are shown in the supporting information (Figure S1, S2, S3, S4, S5, S6). These films were used for the subsequent investigations. Figure 1 shows results of live/dead staining used in conjunction with CLSM to assess the biofilm growth capacity on CS-GO nanocomposite films. In this experiment, CS-GO-0.25% and CS-GO-0.6% were selected to represent medium and high concentrations of GO in the CS-GO nanocomposite. The sludge microbial community in synthetic wastewater was incubated with the nanocomposites for up to 6 d to allow mature biofilms to form. As seen in Figure 1, for pure chitosan films, the CLSM images show that most cells are green, which indicate a healthy growing biofilm on the chitosan surface. Even though, chitosan has been previously described to have antimicrobial properties, in this study, chitosan did not present any toxicity to microorganisms. Previous studies have shown that the antimicrobial activity of chitosan is pH dependent, *i.e.* chitosan displays better antibacterial activity in acidic environments rather than neutral.[18] At pH values below the chitosan pKa (pH = 6.3), the positively charged NH_2 groups of chitosan can interact with the bacterial cell surface by damaging the cell membrane and leading to leaking of intracellular constituents and cell death.[19] However, in this study, the pH of the activated sludge and synthetic wastewater were kept at 7.5, which led to a significant proportion of uncharged NH_2 groups in the chitosan, which reduced the toxicity of chitosan to the wastewater microorganisms.

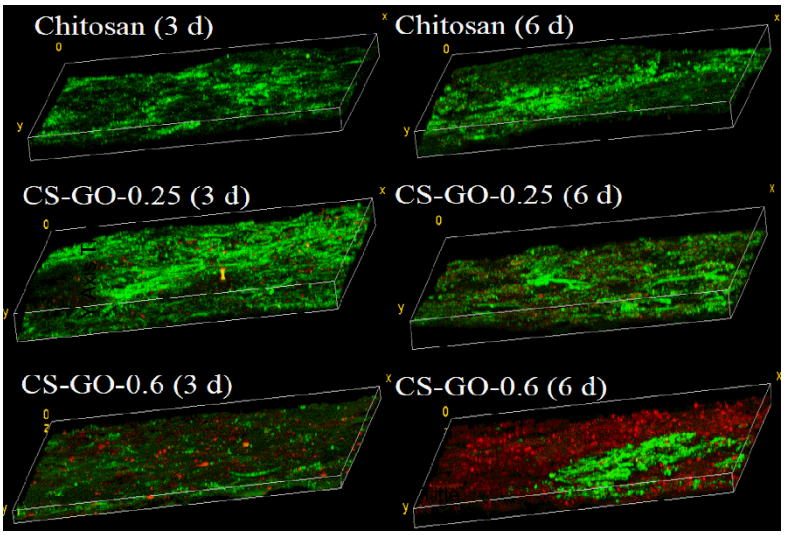

Figure 1: CLSM images of biofilms grown for 3 and 6 d on Chitosan (control), CS-GO-0.25% and CS-GO-0.6% nanocomposite films. The biofilms were stained with SYTO9 and PI prior to microscopic observation. The red colour corresponds to damaged cells, while green correspond to healthy cells. Experiments were run at 25ºC under static conditions.

Compared to chitosan films, increasing numbers of damaged cells were observed in the biofilms grown on CS-GO-0.25% and CS-GO-0.6% nanocomposite films after 6 d (Figure 1). The nanocomposites with higher concentrations of GO exhibited higher toxicity to the biofilms, since more red cells were observed on CS-GO-0.6% than on CS-GO-0.25%. Consequently, the antimicrobial properties exhibited by the CS-GO nanocomposites surfaces could be attributed to the increasing inclusion of GO in the nanocomposite. This result is consistent with other studies using pure cultures of *E. coli* and *B. subtilis*, which proved that the antibacterial effect of CS-GO nanocomposite is dependent on the GO concentration.[20, 21]

Additional insight about the anti-biofilm property of CS-GO nanocomposites with higher GO concentrations could be attained by observations of architectural changes in the biofilms (Figure 1). In the control sample, the biofilm was smooth, thick and homogeneous, while a thinner and more irregular landscape was observed with the nanocomposite films. Previous molecular investigation studies of biofilm development revealed that the formation of biofilms is a complex and dynamic process that involves multiple and convergent signalling pathways.[22] Studies discovered that cell-cell communication through quorum sensing influence the formation of mature biofilms.[23] Hence, in this study, the clear inactivation of cells on the surface of CS-GO-0.6 nanocomposite may be due to the interrupted quorum sensing systems, which led to thinner biofilms on CS-GO-0.6% films, comparing with CS and CS-GO-0.25% films.

The 3-dimensional analysis of the biofilm with COMSTAT allowed us to determine the total biofilm mass, dead biomass, inactivation percentage and average thickness of the biofilms. These biofilm properties are summarized in Table 1.

The total biofilm mass, or total biomass, represents the volume of the biofilm per unit area. The total biomass estimates the biomass attached to the substratum. In our experiments, the total biomass for CS-GO-0.6% was found to be around 50% less than the biomass for CS-GO-0.25% after 3 d of incubation. This trend was maintained even after 6 d. This toxicity dependency on concentration of GO in the nanocomposite is consistent with other graphene-based nanocomposite materials previously reported.[24, 25] The results in Table 1 also shows a slightly decrease in biofilm biomass from 3 to 6 d of incubation. These results are not statistically significant; however, these initial results show a similar trend to other studies with planktonic cells related to time exposure dependency. It is possible that longer exposure of the biofilm to the nanocomposite, would cause a higher and more significant inactivation of the microbial cells in the biofilm. The time exposure dependency of the toxic effect for GO on bacterial cells has been previously observed with other carbon-based nanomaterials.[26]

Table 1 Confocal microscopy data for biofilm growth for 3 and 6 d on CS-GO-0.25% and CS-GO-0.6% films

Time	Material	Total Biomass ($\mu m^3/\mu m^2$)	Dead Biomass ($\mu m^3/\mu m^2$)	% inactivation	Average Thickness (μm)
3 d	Chitosan	19.63 ± 2.21	0.0023 ± 0.00096	0.12 ± 0.0045	33.96 ± 5.53
	CS-GO-0.25%	20.42 ± 2.73	0.0029 ± 0.0011	0.14 ± 0.0037	23.04 ± 1.22
	CS-GO-0.6%	10.74 ± 1.84	3.65 ± 0.05	34.09 ± 1.67	15.19 ± 0.28
6 d	Chitosan	19.85 ± 0.64	0.0021 ± 0.0039	0.10 ± 0.0082	36.29 ± 5.10
	CS-GO-0.25%	13.21 ± 1.19	0.83 ± 1.57	6.31 ± 2.02	26.83 ± 1.74
	CS-GO-0.6%	8.25 ± 4.36	4.18 ± 2.95	50.63 ± 12.51	18.025 ± 2.88

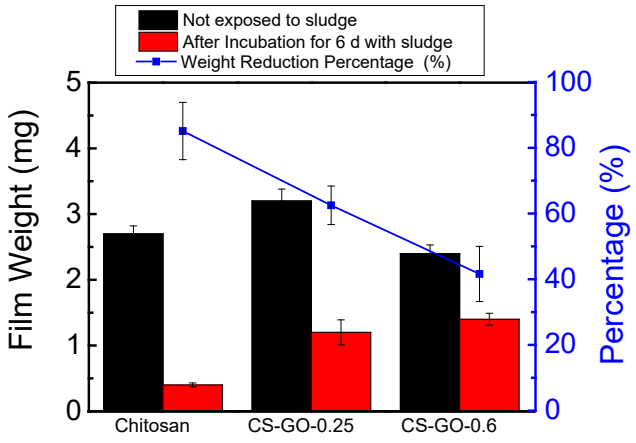

Figure 2 Weight loss of CS-GO nanocomposites before and after incubation for 6 d with wastewater sludge. Error bars in the graph correspond to standard deviations of triplicate samples.

In addition to the total biomass changes, table 1 also shows total microbial inactivation in the biofilm. The results showed that the control samples of chitosan films did not present significant microbial inactivation in the biofilm. However, 35% and 50% inactivation was observed after 6 d of incubation with CS-GO-0.25% and CS-GO-0.6%, respectively. Similarly, as observed with the total biomass, the thickness of the biofilms decreased with increasing content of GO embedded in the films. The overall average biofilm thickness after 6d of incubation, however, increased as compared to the 3 d of incubation for CS-GO-0.25%. This observation could be due to different possibilities; the first one could be that some microorganisms in the biofilm are not sensitive to GO and are able to grow on the surface of the films. Previous investigation has shown that some microorganisms in wastewater are not sensitive to GO and they can grow in the presence of GO.[11] More than that, unlike CS-GO-0.6, the GO content in CS-GO-0.25% might not be high enough to disrupt the biofilm formation process, leading to a higher biofilm thickness after 6 d. Alternatively, it is possible that the microorganisms that died could have served as a layer of protection against GO, allowing a biofilm to form on top of the dead layer of microorganisms. This phenomenon was also previously observed with coatings containing single walled carbon nanotubes.[27] The last possibility seems very plausible with the data observed in Figure 1 and Figure S7 on CS-GO-0.25%. In those figures, it is clear the cells in direct contact with the nanocomposite surface were inactivated more, and some healthy biofilm was still able to grow on the top of dead cells.

Physicochemical changes of the CS-GO films in the sludge: Indication of polymer biodegradation

In addition to the biofilm growth investigation on the films, we also investigated the physico-chemical changes on the CS-GO nanocomposites and chitosan films caused by the biofilm growth. Previous investigations have shown that chitosan is biodegradable by wastewater microbial communities.[28, 29] Thus, we first measured the weight loss of the nanocomposite films after wastewater interaction. As shown in Figure 2, the chitosan film weight reduced by 80%; while 62.5% and 41.6% of weight loss were observed for CS-GO-0.25% and CS-GO-0.6% films, respectively. These results clearly show that the nanocomposites can be biodegraded. It is important to note that the higher the concentration of GO in the nanocomposite, the smaller was the film weight loss (Figure. 2). This result correlates well with the fact that there was higher inactivation of microorganisms in the films with higher GO concentrations (Table 1), which led to fewer active microbes in the biofilm and, therefore, reduced biodegradation of the nanocomposites

In addition to determining nanocomposite weight loss, the chemical changes on the surface of the nanocomposite was investigated through FTIR spectroscopy. This technique was employed to determine the disappearance or formation of new functional groups in the CS-GO nanocomposites and chitosan films (Figure 3).

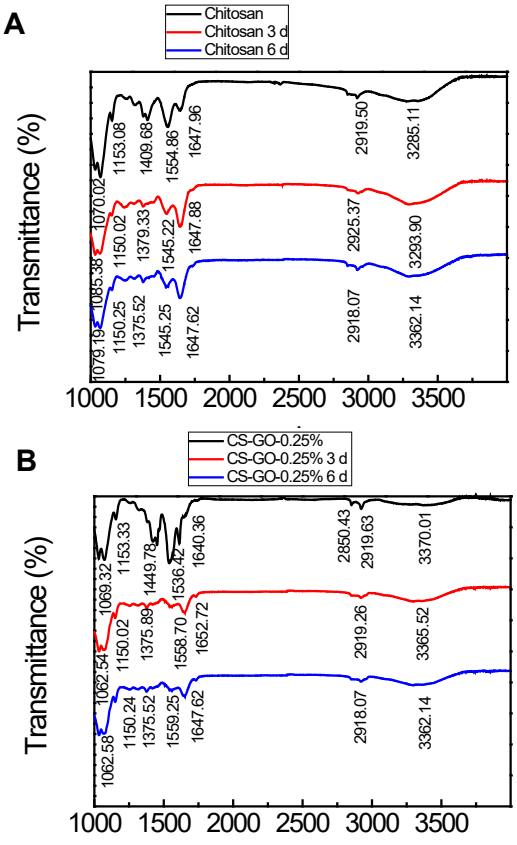

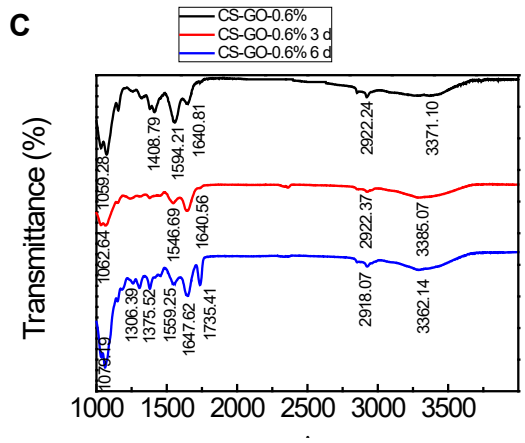

Figure 3 FTIR analysis for CS-GO nanocomposites before and after interaction with microorganisms in the biofilm.

The spectrum of pure chitosan, after 3 d of incubation, showed the appearance of a sharper peak at 1647 cm^{-1}. This peak is attributed to the change of amide I groups, a basic functional group found in protein produced by microbial growth on chitosan films.[30] Even though, we cleaned the biofilms from the surface of the films, clearly some microbial protein remained on the surface. This is supported by a previous study that showed a high degree of film biodegradation accompanied by growth of microorganisms on chitosan films. The biodegradation was attributed to increasing secretion of enzymes, such as chitosanases, which led to increasing emergence of the peak at 1647 cm^{-1}.[31] Similar trends were also observed in other polymer biodegradation studies with mixed bacterial cultures.[32] They observed a peak increase at around 1649 cm^{-1} in their spectrum and explained that this change was due to the formation of β-diketone structures and methyl groups by the scission of several carbon-carbon bonds due to microbial degradation.[33] The intensity of the peaks at 1150 cm^{-1} decreased and was attributed to the breaking of the osidic bridges C-O-C of the glycosidic units after degradation by microorganisms.[29] Other peaks at 1409 and 1545 cm^{-1} also became weaker after microbial exposure, which also supports the occurrence of chitosan degradation.

In Figure 3 (B), the peaks on the spectra of CS-GO-0.25%, after interaction for 3 and 6 d with activated sludge, were similar to pure chitosan. This might be due to the low content of GO in CS-GO-0.25%. However, for CS-GO-0.6% (Figure 3 (C)), changes on the FITR spectra of CS-GO-0.6% films exposed for 3 and 6 d to activated sludge were observed. New peaks appeared at 1306 and 1375 cm^{-1}. These peaks correspond to stretching vibrations of C-O-C bonds from epoxy or alkoxy; and to C-OH bonds typically found in GO. In addition, the characteristic peak of C=O stretching at 1735 cm^{-1}, which corresponds to the carboxylic group of GO was obvious in the spectrum after 6 d. The appearance of GO peaks on the surface of the nanocomposite after 6 d suggests the emergence of GO on the surface of the nanocomposite due to the biodegradation of the chitosan surrounding the nanomaterial. The spectrum for CS-GO nanocomposites exposed to wastewater without sludge is shown in the supporting information. There were no clear changes for CS-GO nanocomposites after 6 d of incubation. This proved that the appearance of GO was due to the biodegradation of chitosan. The SEM image (Figure 4) also confirms this finding. As shown in Figure 4, the original nanocomposite surface was clearly covered by chitosan, which made the surface smooth and homogenous. After 6 d of incubation with the activated sludge, GO platelets are clearly exposed. These results confirm that the microorganisms are able to biodegrade the polymer and expose GO.

It has been reported that some bacteria could efficiently use chitosan as a carbon source by producing chitosanases to degrade chitosan into glucosamine oligomers.[28, 34] Therefore, it is plausible to hypothesize that chitosan on top of GO was degraded by the activated sludge microbial community and used as carbon source. From the results, however, GO did not seem to have been degraded in the duration of this experiment. It is possible that it can still be biodegraded, but might have a slower biodegradation rate compared to chitosan.[35, 36]

Toxicity behaviour of CS-GO during biodegradation

Reports in the literature state that GO is toxic to microorganisms by direct contact between the sharp edges of GO nanosheets and the microorganisms, as well as by production of reactive oxygen species (ROS).[37, 38] To determine the evolution of these known toxic mechanisms before and after biodegradation, we determined the surface morphology changes of the films as well as the production of ROS after biodegradation of the nanocomposites.

Change in Surface morphology of the CS-GO films after biodegradation

The change in surface roughness of the nanocomposites was evaluated through AFM before and after exposure to sludge. As seen in Figure 5, the R_a for pure chitosan films at 0 and 6 d of incubation did not change significantly. For CS-GO films, the roughness increased 2.8 and 2.4 times after biodegradation of the CS-GO-0.25% and CS-GO-0.6% nanocomposites, respectively. This increase in roughness was attributed to the emergence of GO after biodegradation of the polymer. This increasing emergence of GO allowed the exposure of sharp edges of GO on the surface of the nanocomposite film. It has been well demonstrated that GO disturbs primarily the cell membrane by direct contact with bacteria.[38] Hence, AFM, as a supplemental method to SEM (Figure 4), suggests that the biodegradation of the nanocomposite leads to the appearance of sharper edges of GO on the surface of the nanocomposite. This appearance of the GO on the surface could have led to mechanical damage of the cells, which would explain the anti-biofilm effect of CS-GO nanocomposites after 6 d, when the chitosan on top of the film got degraded.

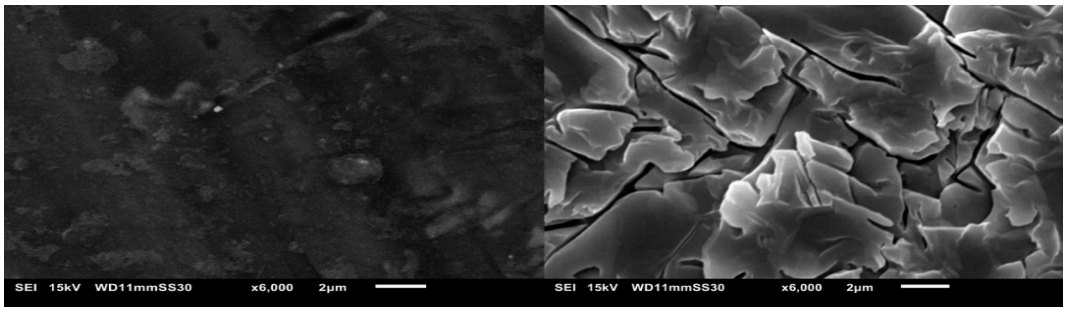

Figure 4 SEM of CS-GO-0.6% nanocomposites before and after 6 d of interaction with activated sludge.

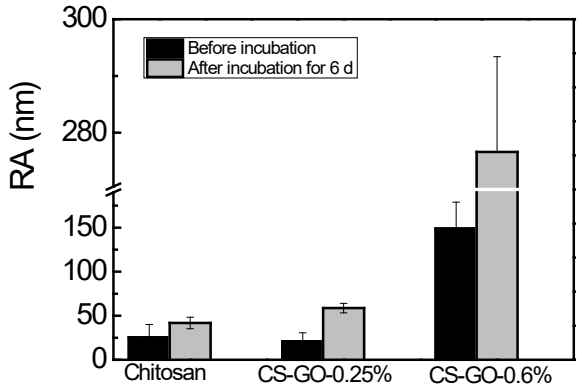

Figure 5 Average roughness of CS-GO nanocomposite surfaces before and after the biofilm interaction.

Increasing ROS production with increasing exposure of GO on the surface

Earlier, the results showed that with higher concentrations of GO embedded in the polymer matrix, the appearance of GO on the surface occured more readily. The emergence of GO clearly led to anti-biofilm properties. Production of ROS is often suggested as a key antibacterial mechanism for carbon based nanomaterials, including GO.[4, 39] Therefore, in this present study, we used the thiol oxidation assay to evaluate the generation of ROS on CS-GO nanocomposites before and after sludge interaction.

In the thiol oxidation assay, pure chitosan films were used as negative controls, while a H_2O_2 solution was the positive control. For the chitosan films before and after sludge exposure, the results showed that the films generated negligible H_2O_2. In the case of nanocomposites, the increasing percentage of GO dispersed in the nanocomposites led to increasing generation of H_2O_2 (Figure 6). The highest oxidation capacity (86.72%) towards GSH was observed with CS-GO-0.6% films, which was 20.2 times higher than the chitosan films. The results of the concentration-dependency of oxidation capacity were consistent with the antibacterial activity observed in Figure 5. Carpio et al. also demonstrated that the antibacterial activity of GO is time and concentration dependent. [24, 38] Therefore, more GSH will be oxidized with increasing GO concentration. This trend is also consistent in this study, which showed that CS-GO-0.6% presented higher GSH oxidation capacity.

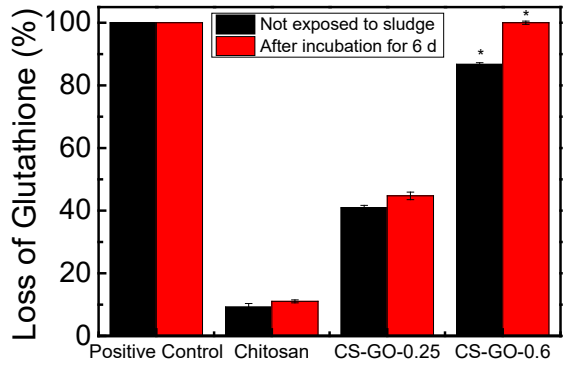

Figure 6 Loss of glutathione of CS-GO nanocomposites before and after incubation for 6 d with wastewater. The symbol * corresponds to statistically different results between the chitosan films and the nanocomposite samples with a 95% confidence interval.

After interaction with sludge, a noticeable increase in loss of glutathione was observed with the nanocomposites. This loss was more pronounced in the CS-GO-0.6% nanocomposite. This result is supported by the emergence of GO after chitosan biodegradation in the nanocomposite (Figures 4 and 5). These results suggest that the toxicity of GO can be attributed to generation of ROS. The current accepted mechanism is that the unpaired electrons of GO reduce molecular oxygen to form $\bullet O_2^-$. The $\bullet O_2^-$ can react with the hydrogen atom to produce H_2O_2. The ROS generation from GO has also been attributed to the presence of functional groups. Since GO contains abundant hydroxyl groups, these hydroxyl groups can get detached from GO to form •OH. GO can then catalyze the formation of •OH from H_2O_2.[39, 40] In this study, similar mechanism could be proposed for CS-GO nanocomposites since chitosan did not contribute to the anti-biofilm property of the nanocomposite.

Hence, the nanocomposite degradation and anti-biofilm property observed in this study showed that the biopolymer, chitosan, coating the top of nanocomposite films will be degraded first by the microbial community. The biopolymer used as carbon source allows the initial proliferation of the biofilm. After biodegradation of the chitosan, the GO gets exposed and interacts with the biofilm, causing cell inactivation by ROS activity and mechanical disruption.

Conclusions

CS-GO nanocomposites started to present anti-biofilm properties between 3 to 6 d of interaction with the activated sludge. The exposure time and concentration of the GO embedded in the nanocomposite played an important role in the toxicity observed for CS-GO nanocomposites. The amount of time for the nanocomposite to show toxic effects was directly related to the amount of time necessary for the microorganisms in the sludge to degrade the polymer and expose GO on the surface of the film. The exposed GO from the films were able to readily inactivate the microorganisms on the surface by reactive oxidative stress production and physical cell disruption by the sharp edges of GO. The pure chitosan did not manifest any antimicrobial properties and was able to biodegrade easily throughout the experiments. In terms of broader environmental implications and life cycle of nanocomposites, this investigation reveals that biodegradable polymers used to synthesize nanocomposites can still be partially biodegraded depending on the concentration of the anti-microbial nanomaterial. It is possible, however, that during biodegradation, the nanoparticles present in the nanocomposites are released to the environment and could potentially cause hazardous effects to health and environment. Hence, further investigations for the release of these nanoparticles to the environment should be done to determine the proper disposal of nanocomposites.

Acknowledgements

This project was made possible through the funding from the Texas Hazardous Waste Research Center (THWRC Project Award #: 515UHH0049H) and partial funding from the National Science Foundation Career Award (NSF Award #1150255).

References

1. J. Ma, C. Liu, R. Li and J. Wang, *Journal of Applied Polymer Science*, 2012, **123**, 2933-2944.
2. H. N. Lim, N. M. Huang and C. Loo, *Journal of Non-Crystalline Solids*, 2012, **358**, 525-530.

3. F. Hussain, M. Hojjati, M. Okamoto and R. E. Gorga, *Journal of composite materials*, 2006, **40**, 1511-1575.
4. J. Fan, Y. Li, H. N. Nguyen, Y. Yao and D. F. Rodrigues, *Environmental Science: Nano*, 2015, **2**, 370-379.
5. J. K. Pandey, K. R. Reddy, A. P. Kumar and R. Singh, *Polymer degradation and stability*, 2005, **88**, 234-250.
6. A. Göpferich, *Biomaterials*, 1996, **17**, 103-114.
7. V. K. Rana, M. C. Choi, J. Y. Kong, G. Y. Kim, M. J. Kim, S. H. Kim, S. Mishra, R. P. Singh and C. S. Ha, *Macromolecular Materials and Engineering*, 2011, **296**, 131-140.
8. L. Shao, X. Chang, Y. Zhang, Y. Huang, Y. Yao and Z. Guo, *Applied Surface Science*, 2013, **280**, 989-992.
9. Y. Pranoto, S. Rakshit and V. Salokhe, *LWT-Food Science and Technology*, 2005, **38**, 859-865.
10. J. V. D. Perez, E. T. Nadres, H. N. Nguyen, M. L. P. Dalida and D. F. Rodrigues, *RSC Advances*, 2017, **7**, 18480-18490.
11. H. N. Nguyen, S. L. Castro-Wallace and D. F. Rodrigues, *Environmental Science: Nano*, 2017.
12. I. E. Mejias Carpio, C. M. Santos, X. Wei and D. F. Rodrigues, *Nanoscale*, 2012, **4**, 4746-4756.
13. J. M. Carlos David Grande, Jingjing Fan, Al De Leon, J. G. R. Johannes Delgado-Ospina, Debora F. Rodrigues, R. Advincula and *Macromolecular Symposia - MACROMEX 2014*, 2017.
14. R. P. Medina, E. T. Nadres, F. C. Ballesteros and D. F. Rodrigues, *ES: Nano*, 2016, **3**, 638-646.
15. K. A. Third, M. Newland and R. Cord‐Ruwisch, *Biotechnology and Bioengineering*, 2003, **82**, 238-250.
16. D. F. Rodrigues and M. Elimelech, *Environmental science & technology*, 2010, **44**, 4583-4589.
17. J. Fan, T. O. Okyay and D. F. Rodrigues, *Journal of hazardous materials*, 2014, **279**, 236-243.
18. M. Kong, X. G. Chen, K. Xing and H. J. Park, *International journal of food microbiology*, 2010, **144**, 51-63.
19. S. C. Motshekga, S. S. Ray, M. S. Onyango and M. N. B. Momba, *Applied Clay Science*, 2015, **114**, 330-339.
20. H. N. Lim, N. M. Huang and C. H. Loo, *Journal of Non-Crystalline Solids*, 2012, **358**, 525-530.
21. K. Sundar, V. Harikarthick, V. S. Karthika and A. Ravindran, *Journal of Bionanoscience*, 2014, **8**, 207-212.
22. Y.-H. Li, N. Tang, M. B. Aspiras, P. C. Lau, J. H. Lee, R. P. Ellen and D. G. Cvitkovitch, *Journal of bacteriology*, 2002, **184**, 2699-2708.
23. M. Simões, L. C. Simões and M. J. Vieira, *LWT - Food Science and Technology*, 2010, **43**, 573-583.
24. S. Liu, T. H. Zeng, M. Hofmann, E. Burcombe, J. Wei, R. Jiang, J. Kong and Y. Chen, *ACS Nano*, 2011, **5**, 6971-6980.
25. C. M. Santos, M. C. R. Tria, R. A. M. V. Vergara, F. Ahmed, R. C. Advincula and D. F. Rodrigues, *Chemical Communications*, 2011, **47**, 8892-8894.
26. F. Ahmed, C. M. Santos, R. A. M. V. Vergara, M. C. R. Tria, R. Advincula and D. F. Rodrigues, *Environmental science & technology*, 2012, **46**, 1804-1810.
27. D. F. Rodrigues and M. Elimelech, *Environ Sci Technol*, 2010, **44**, 4583-4589.
28. X.-A. Gao, W.-T. Ju, W.-J. Jung and R.-D. Park, *Carbohydrate Polymers*, 2008, **72**, 513-520.
29. M. Kammoun, M. Haddar, T. K. Kallel, M. Dammak and A. Sayari, *International journal of biological macromolecules*, 2013, **62**, 433-438.
30. C. Z. Kibédi-Szabó, M. Stroescu, A. Stoica-Guzun, S. I. Jinga, S. Szilveszter, I. Jipa and T. Dobre, *Journal of Polymers and the Environment*, 2012, **20**, 422-430.
31. D. Klemenčič, B. Simončič, B. Tomšič and B. Orel, *Carbohydrate polymers*, 2010, **80**, 426-435.
32. X. Pang and C.-C. Chu, *Biomaterials*, 2010, **31**, 3745-3754.
33. H. Z. Zhang, *Journal of Polymers and the Environment*, 2009, **17**, 286-290.
34. M. Shimosaka, M. Nogawa, X. Wang, M. Kumehara and M. Okazaki, *Applied and environmental Microbiology*, 1995, **61**, 438-442.
35. J.-T. Chen, Y.-J. Fu, Q.-F. An, S.-C. Lo, Y.-Z. Zhong, C.-C. Hu, K.-R. Lee and J.-Y. Lai, *Carbon*, 2014, **75**, 443-451.
36. R. Justin and B. Chen, *Carbohydrate polymers*, 2014, **103**, 70-80.
37. A. Ammar, A. M. Al-Enizi, M. A. AlMaadeed and A. Karim, *Arabian Journal of Chemistry*, 2016, **9**, 274-286.
38. I. E. M. Carpio, C. M. Santos, X. Wei and D. F. Rodrigues, *Nanoscale*, 2012, **4**, 4746-4756.
39. E. T. Nadres, J. Fan and D. F. Rodrigues, in *Graphene-based Materials in Health and Environment*, Springer, 2016, pp. 323-356.
40. C. Su, M. Acik, K. Takai, J. Lu, S.-j. Hao, Y. Zheng, P. Wu, Q. Bao, T. Enoki and Y. J. Chabal, *Nature communications*, 2012, **3**, 1298.

ARTICLE